Journal of Hydrology 560 (2018) 461–470

Contents lists available at ScienceDirect

Journal of Hydrology

journal homepage: www.elsevier.com/locate/jhydrol

Research papers

Decadal changes of reference crop evapotranspiration attribution: Spatial and temporal variability over China 1960–2011

Ze-Xin Fan [a], Axel Thomas [b,*]

[a] Key Laboratory of Tropical Forest Ecology, Xishuangbanna Tropical Botanical Gardens, Chinese Academy of Sciences, Mengla, Yunnan 666303, China
[b] GIS Service GmbH, 55263 Wackernheim, Germany

ARTICLE INFO

Article history:
Received 21 June 2017
Received in revised form 26 February 2018
Accepted 27 February 2018
Available online 6 March 2018
This manuscript was handled by T. McVicar, Editor-in-Chief, with the assistance of Yuting Yang, Associate Editor

Keywords:
Climate change
Temporal and spatial variability of attribution
FAO-Penman-Monteith reference crop evapotranspiration
China

ABSTRACT

Atmospheric evaporative demand can be used as a measure of the hydrological cycle and the global energy balance. Its long-term variation and the role of driving climatic factors have received increasingly attention in climate change studies. FAO-Penman-Monteith reference crop evapotranspiration rates were estimated for 644 meteorological stations over China for the period 1960–2011 to analyze spatial and temporal attribution variability. Attribution of climatic variables to reference crop evapotranspiration rates was not stable over the study period. While for all of China the contribution of sunshine duration remained relatively stable, the importance of relative humidity increased considerably during the last two decades, particularly in winter. Spatially distributed attribution analysis shows that the position of the center of maximum contribution of sunshine duration has shifted from Southeast to Northeast China while in West China the contribution of wind speed has decreased dramatically. In contrast relative humidity has become an important factor in most parts of China. Changes in the Asian Monsoon circulation may be responsible for altered patterns of cloudiness and a general decrease of wind speeds over China. The continuously low importance of temperature confirms that global warming does not necessarily lead to rising atmospheric evaporative demand.

1. Introduction

Atmospheric evaporative demand (AED) refers to the combined evaporation and transpiration over a land surface, which plays an essential role in global atmosphere-hydrosphere-biosphere interactions (Huntington, 2006), and influences fundamental properties of terrestrial ecosystems such as runoff, soil moisture and plant growth (Fisher et al., 2011). AED encompasses different concepts of evapotranspiration (ET): estimates of potential evapotranspiration (ET_p) and reference crop evapotranspiration (ET_0) as well as measured pan evaporation (E_{pan}).

ET_p describes evaporation from an open water surface (Penman, 1948, Shuttleworth, 1993). The Penman formulation is a physically based formulation that encompasses all meteorological variables that govern the evaporative process. ET_0 is an extension of the original Penman formulation (Monteith, 1965) estimating the combined water loss from soil and vegetation. The FAO Penman-Monteith (FAO-PM) formulation (Allen et al., 1998), initially developed to estimate crop water and irrigation requirements, has been used in many of the studies dealing with AED changes (e.g. Azorin-Molina et al., 2015). E_{pan} in contrast is an actual measurement of AED with the help of evaporation pans (Smith, 1975).

All three concepts assume an unlimited water supply and are a measure of the maximum amount of water transferred to the atmosphere under given meteorological conditions. Only in humid (not water-limited) environments will they directly give a reliable estimate of the actual water loss to the atmosphere. However, a complete investigation into the causes of actual ET rates would require considering a number of factors (i.e. precipitation, soil characteristics, vegetation cover and land use, among others). The restriction of standardized conditions focusing exclusively on the meteorological factors of AED alone makes it an ideal tool to analyze and compare AED in different climates worldwide.

Milly and Dunne (2016) noted differences between GCM results and AED estimates that are thought to come from the lack of adaption of stomatal conductance reductions to increasing atmospheric CO_2 concentrations. In general there is a fair agreement between GCM results and ET_0 estimates (Scheff and Frierson, 2014). While GCM experiments are based on non-linear physical models, the ET_0 formulation uses only fixed land surface parameters to simulate

* Corresponding author.
E-mail address: axel.thomas@gisservice-gmbh.de (A. Thomas).

https://doi.org/10.1016/j.jhydrol.2018.02.080
0022-1694/

the effects of a crop cover on AED. If results of GCM experiments do represent a fair approximation of AED this would indicate a systematic bias in AED estimates with atmospheric CO_2 concentration. However, only if century scale changes are considered do differences amount to 0.03–0.5 mm d^{-1} (Milly and Dunne, 2016). For the much shorter time periods commonly considered in AED attribution analysis a fixed stomatal conductance would likely not introduce noticeable errors. Any errors would be further reduced by the smoothing effect of the regression equation used for the attribution analysis.

In a warming climate, where a warmer atmosphere will be able to hold more water and hence potentially allow for higher AED, the hydrological cycle is expected to intensify (IPCC, 2013). However, despite globally increasing temperatures, most studies have shown that measured E_{pan} and calculated ET_0 rates are declining at both global and regional scales, mainly due to reduction in terrestrial wind speeds and solar radiation levels (Peterson et al., 1995; Roderick and Farquhar, 2002; Liu et al., 2004; Roderick et al., 2009; McVicar et al., 2012). This contradiction is known as "pan evaporation paradox" (Brutsaert and Parlange, 1998).

A correct understanding of temporal and spatial changes of AED rates in a warming climate has far reaching consequences not only for climate science in general but also for forecasting future AED rates and developing suitable mitigation strategies for the projected stress on water supplies and agriculture. This is of special concern in China, which feeds 22% of the world's population from only 7% of the world's arable land (Piao et al., 2010). With a large percentage of the farmland used for water-consuming rice crops as well as vast tracts in semiarid areas with high irrigation demand, the precise knowledge of AED rates and its potential future development is of prime importance.

ET_0 trends in China have decreased in general but have shown large spatial variations both in trend direction and magnitude (Thomas, 2000; Chen et al., 2005, 2006; Xu et al., 2006a; Wang et al., 2007; Zhang et al., 2007, 2009; Liu et al., 2010; Song et al., 2010; Yin et al., 2010a; Tang et al., 2011; Li et al., 2014). Attribution studies have analyzed to which extent the climatic variables governing AED (solar radiation, wind speed, relative humidity and air temperature) lead to the observed ET_0 rates. Decreasing solar radiation ('global dimming', Li et al., 1998; Wild et al., 2005) and diminishing wind speeds ('stilling', Xu et al., 2006b, Vautard et al., 2010) have been cited as the major cause (Thomas, 2000; Chen et al., 2006; Xu et al., 2006a; Wang et al., 2007, 2011; Zheng et al., 2009; Liu et al., 2010; Song et al., 2010; Yin et al., 2010a, 2010b;Tang et al., 2011; Liu et al., 2012; Fan and Thomas, 2013; Ye et al., 2014; Huang et al., 2015; Zheng and Wang, 2015; Gao et al., 2016; Liu et al., 2017; Wang et al., 2017). Even the first attribution analysis of ET_0 rates in China (Thomas, 2000) has shown that rising temperatures do not necessarily cause rising ET_0 rates. This is line with results from other regional studies outside of China (McVicar et al., 2012). Variations in regional circulation intensity (Xu et al., 2006b; Gao et al., 2006) or teleconnection patterns (Hartmann et al., 2009) are also likely causes.

A major drawback of all previous attribution studies has been that they analyzed mean climatic values averaged over their entire respective observation periods. The resulting long-term attribution analyses provide no insight into temporal changes that might be related to either natural secular changes or global warming. Time series analysis of attribution is required to obtain new insights into the causes of changing AED.

To study spatiotemporal variability of attribution patterns over several climate zones and a large latitudinal extent, our objectives are: (i) to evaluate the relationships between the driving climatic factors and ET_0 variability; and (ii) to assess their temporal and spatial variation.

2. Study site and data processing

2.1. Climate data preprocessing

A total of 644 meteorological stations, with monthly data for the period 1960–2011 were provided by the Climatic Data Center (CDC) of the National Meteorological Information Center of China (NMIC) (Fig. 1). The dataset includes monthly mean sunshine duration (SD, h), wind speed (WS, m s^{-1}), relative humidity (RH,%) and minimum as well as maximum temperature (TMX, °C). With the exception of the extreme western (western Tibetan Plateau) and northwestern (Gobi and Tarim Basin) parts of the study area, the stations are equally distributed covering an elevational range of 4800 m from 2 m to 4800 m. Climate data were homogenized and missing values were estimated from up to 10 neighboring stations (Peterson et al., 1998) with the R package 'climatol' (R Development Core and Team, 2004; http://www.climatol.eu/index.html). The homogeneity tests are applied on a difference series between the tested station and a reference series constructed as a weighted average of series from nearby stations. This homogenization methodology involves three steps: a type II regression, missing data estimation and outlier and break detection and correlation (Guijarro, 2014).

2.2. Estimation of FAO PM reference crop evapotranspiration rates

The FAO-PM method used in this study has been widely accepted for calculating ET_0 (Allen et al., 1998). In this method, the land cover is defined as a hypothetical reference crop with height of 0.12 m, a fixed surface resistance of 70 s m^{-1} and an albedo of 0.23 (Allen et al., 1998). The FAO-PM equation to estimate ET_0 (mm day^{-1}) is given as:

$$ET_0 = \frac{0.408\Delta(R_n - G) + \gamma \frac{900}{T+273} u_2 (e_s - e_a)}{\Delta + \gamma(1 + 0.34u_2)} \quad (1)$$

where R_n is the net radiation at the crop surface (MJ m^{-2} d^{-1}), G is soil heat flux (MJ m^{-2} d^{-1}), T is mean daily air temperature at 2 m (°C), u_2 is the wind speed at 2 m (m s^{-1}), e_s is saturation vapour pressure (kPa), e_a is actual vapour pressure (kPa), Δis the slope of the saturation vapour pressure curve at air temperature T [kPa $°C^{-1}$] and γ is the psychrometric constant [kPa $°C^{-1}$]. Daily ET_0 values were summed to monthly totals.

Net radiation at the crop surface R_n is a function of solar radiation R_s. With no directly measured R_s available, we relied on the conversion of observed sunshine duration to R_s (Doorenbos and Pruitt, 1977; Allen et al., 1998). R_s can be estimated from observed sunshine duration using the Ångström formula (Ångström, 1924):

$$R_s = \left(a_s + b_s \frac{n}{N}\right) R_a \quad (2)$$

where a_s is the fraction of extraterrestrial radiation on overcast days, $a_s + b_s$ is the fraction of extraterrestrial radiation on clear days, n is the actual duration of sunshine (h), N is maximum possible duration of sunshine (h) and R_a is the extraterrestrial radiation intensity (MJ m^{-2} day^{-1}). In order to derive solar radiation values from observed sunshine duration, we performed regression analysis with directly measured solar radiation data available for a subset of 123 stations available from the National Meteorological Information Centre of China (NMIC). The derived Ångström constants a_s and b_s were spatially interpolated to a raster surface. Interpolation was performed by Kriging with extended drift using elevation as auxiliary predictor and a 1 km DEM dataset in ArcMap 10.0 (ESRI, 2011). The a_s and b_s values for stations without directly measured solar radiation were derived from the raster data sets at the respective station location. The wind speed at 2 m above ground surface was derived from the normal measurement at 10 m based on the

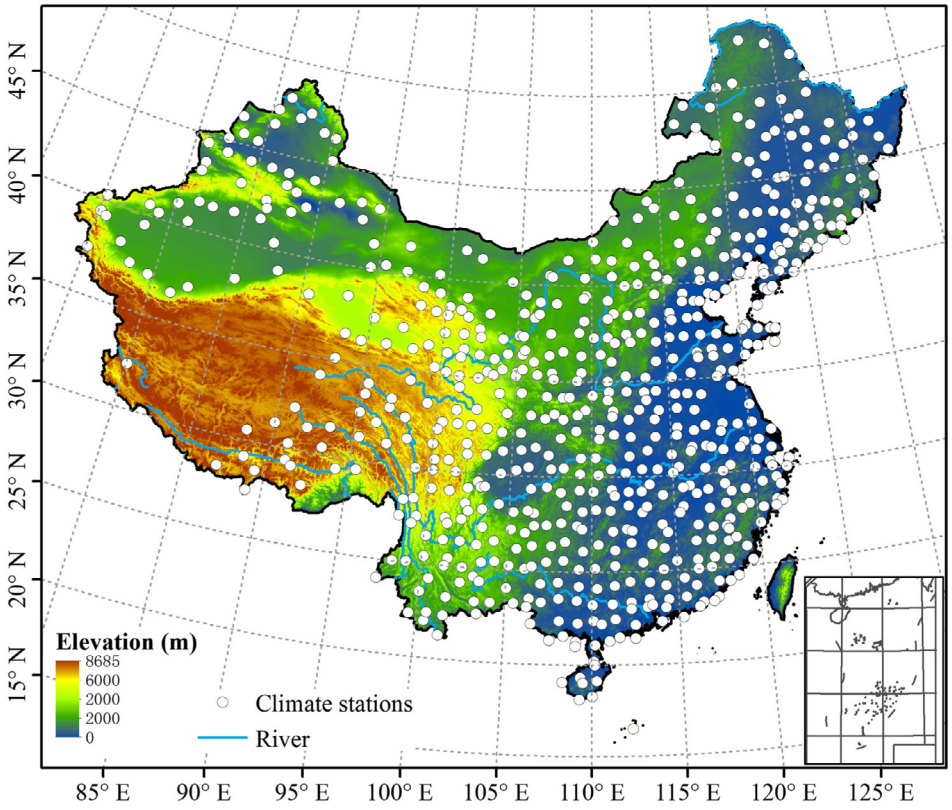

Fig. 1. Location of 644 meteorological stations over China. Blue lines show the major rivers of China. Topographic data derived from 1 km Digital Elevation Model.

logarithmic wind speed profile equation given by (Allen et al., 1998).

3. Methods

3.1. Analysis of relationships between driving climatic factors and ET0 variability

The relationship between ET_0 rates and climatic variables was analyzed with multiple regressions on a monthly basis, with ET_0 as dependent variable and SD, WS, RH and TMX as predictors, using the 'lm' function in R software. Variables were selected into the final model based on the lowest Aikaike Information Criterion, using stepwise backward elimination of predictors. The contribution of each significant variable was determined by explained variance (EV).

3.2. Analysis of temporal and spatial variation of attribution

In order to analyze the temporal variability of the contribution of the individual climatic variables, we further performed stepwise multiple regressions for moving windows of ten years width (1960–1969, 1961–1970,..., 2002–2011), which produces a time series of EV for each station. We also explored the temporal and spatial patterns of EV using a multiple factor analysis (MFA) on monthly values. This ordination technique identifies the common structure among different sets of variables defined for the same individuals (Escofier and Pages, 1994). MFA performs separate principal component analysis (PCA) on each set of variables. The elements of each set are then divided by the square root of the first eigenvalue of each PCA and a global PCA is then performed on the normalized data set. We performed MFA for the EV time series (SD, WS, RH and TMX) for 644 stations, by using the FactoMineR package (Lê et al., 2008) in R 3.23 (R Development Core and Team, 2004). The first six factor loadings resulting from MFA were interpolated with Kriging method using ArcMap software (version 10.0).

4. Results

4.1. Relationships between driving climatic factors and ET0 variability

Values for a_s, b_s and (a_s + b_s) range from 0.13 to 0.32, 0.43 to 0.63 and 0.67 to 0.90, respectively (Fig. 2). Maximum (a_s + b_s) values $\geq$ 0.8 which indicate maximum atmospheric transmittance for very clear days are concentrated above 3000 m a.s.l. in SW and W China. Our modelled a_s and b_s values are in line with Chen et al. (2004) who give very similar values and a comparable spatial distribution.

Averaged over the entire observation period (1960–2011) the four climatic factors (SD, WS, RH and TMX) accounted for almost 80% of annual ET_0 variation over China, with higher EV in West China than in East China (Fig. 3). In general SD explained the highest variance (on average 32%), with RH, WS and TMX each explaining consecutively less EV (Table 1).

At seasonal time scales spatial patterns of EV showed that SD was the most important climatic factor determining ET_0 rates in eastern China and during spring and summer season (Table 1, Fig. 4a and b). In contrast WS was important for ET_0 changes in the arid desert areas of Northwest China during autumn and on the southern Tibetan Plateau during winter season (Fig. 4c and d). RH explained the highest variance during autumn and winter seasons (average EV up to 47%), while with the exception of northwestern China in spring (Fig. 4a). TMX EV remained low throughout the entire study area.

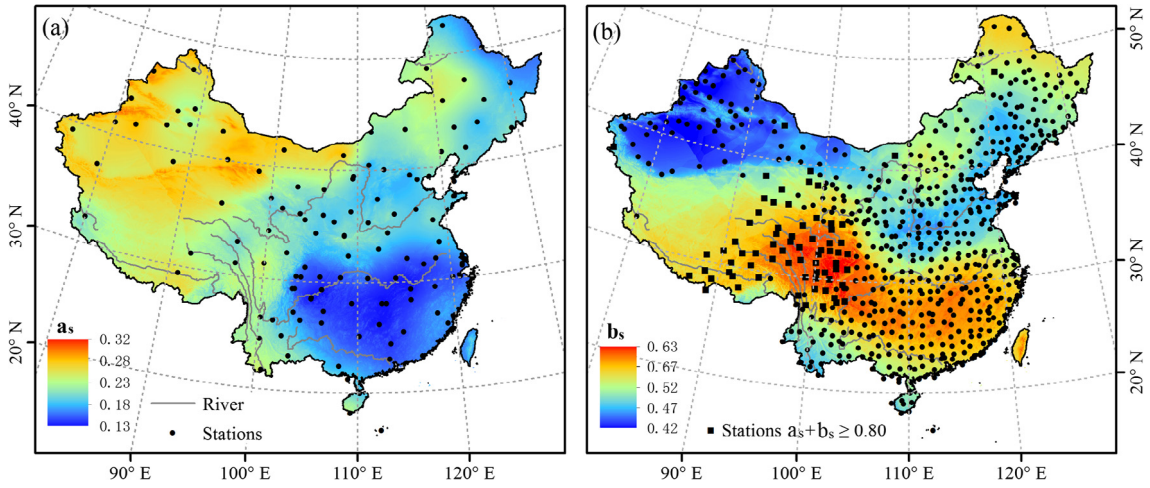

Fig. 2. Spatial distribution of the coefficient a_s (Fig. 2a) and b_s (Fig. 2b) interpolated from 123 meteorological stations as shown in Fig. 2a. Coefficients for 644 stations shown in Fig. 2b were derived from interpolated data. Stations with $(a_s + b_s) \geq 0.80$ are marked with squares.

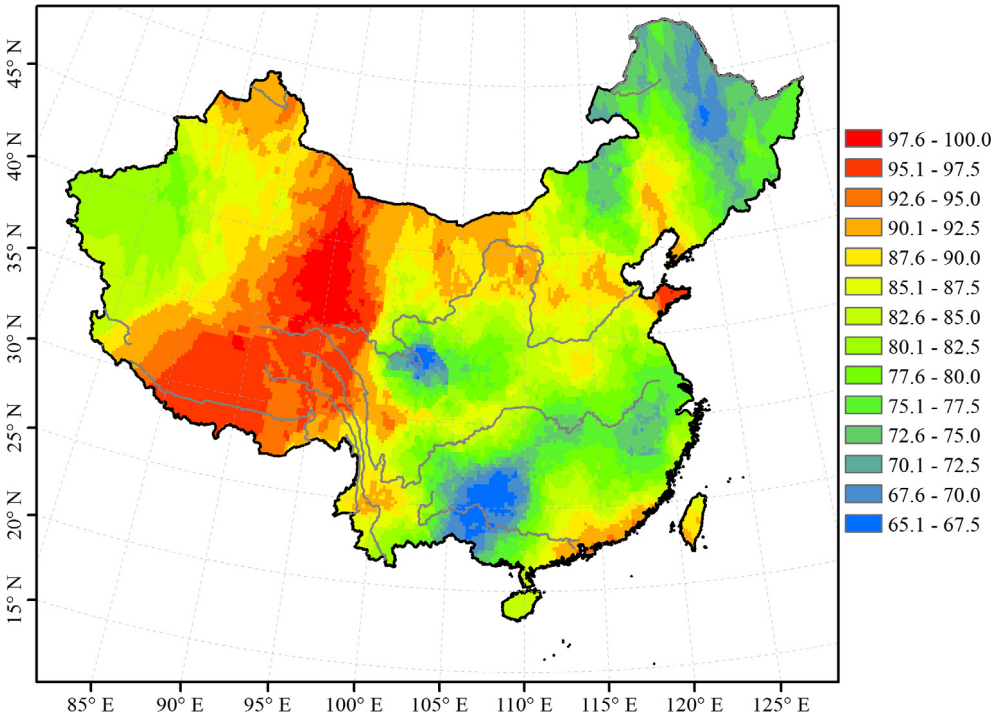

Fig. 3. Spatial patterns of explained variance EV (R^2,%) derived by stepwise multiple regression with annual reference crop evapotranspiration (ET_0) as dependent variable and annual means of sunshine duration (SD), wind speed (WS), relative humidity (RH) and maximum temperature (TMX) as predictors.

Table 1
Statistics of multiple regressions with annual and seasonal reference crop evapotranspiration (ET_0, mm) as dependent variable and relative sunshine duration (SD,%), relative humidity (RH,%), maximum temperature (TMX) and wind speed (WS, m s^{-1}) as predictors. Values are explained variance (%) for each variable averaged for all individual stations. F-Statistic indicates the mean (ranges) of F-statistic of multiple regressions for all stations. The *** represent significance at $p < 0.001$ level.

Season	SD	WS	RH	TMX	Total R^2	F-Statistic
Annual	31.9%	15.4%	21.4%	11.0%	79.7%	56.5 (7.8–258.2)***
Spring	37.1%	12.1%	23.1%	21.1%	93.4%	204.9 (20.8–593.1)***
Summer	55.1%	9.3%	17.6%	15.8%	97.8%	1173.6 (21.1–4526.1)***
Autumn	10.5%	15.3%	37.4%	14.0%	77.1%	54.0 (5.5–271.8)***
Winter	6.0%	13.7%	46.6%	17.1%	83.5%	103.6 (2.7–843.7)***

Temporal attribution variability, as shown by the All-China EV time series (Fig. 5), underlines that over the last 50 years SD always was by far the most important climatic factor explaining ET_0 rates, with RH following on second place. WS and TMX each explained slightly more than 10%. While SD EV remained relatively stable, RH EV experienced a rapid increase in the last two decades;

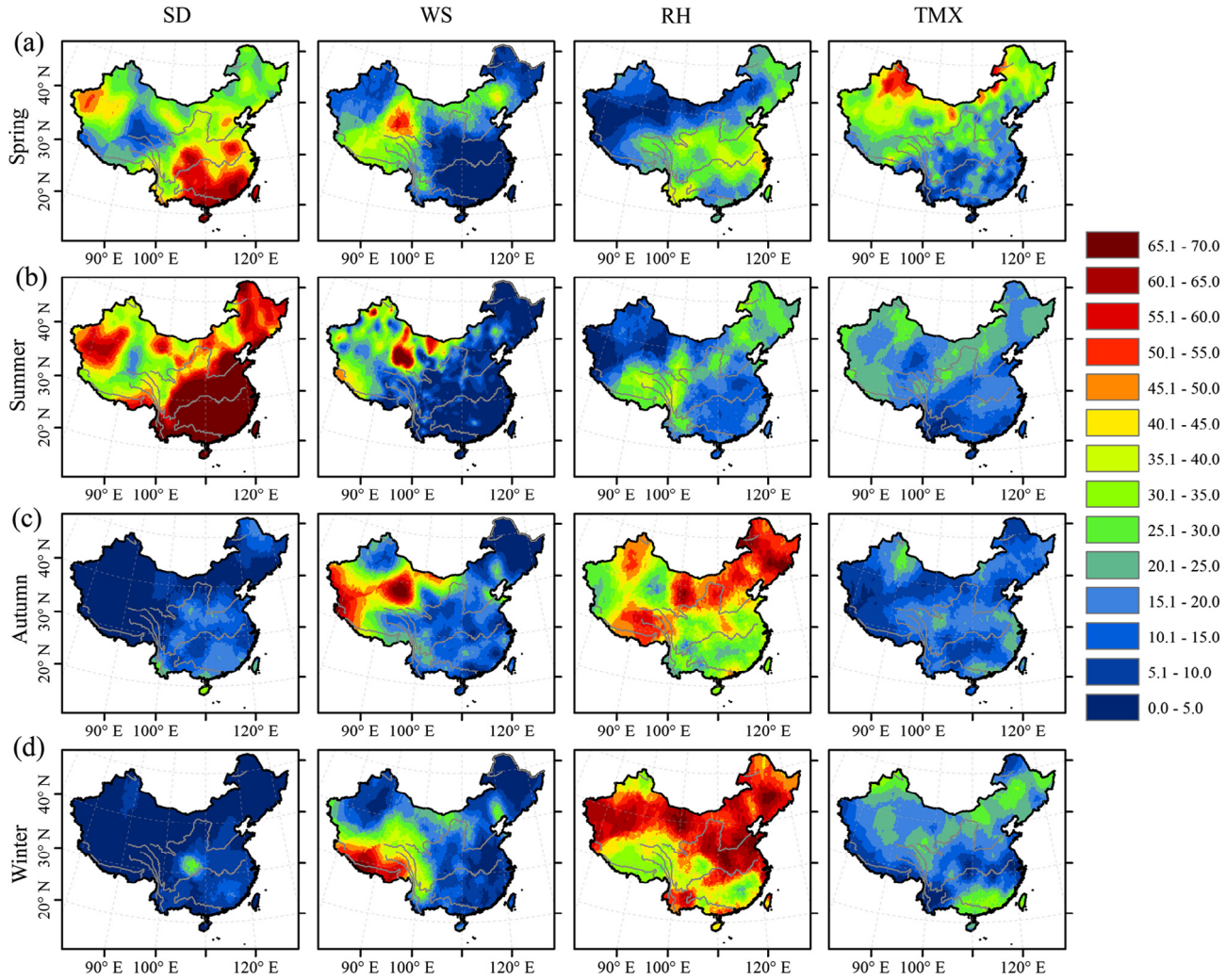

Fig. 4. Spatial patterns of explained variance EV (R^2,%) derived by stepwise multiple regression with seasonal reference crop evapotranspiration (ET_0) as dependent variable and seasonal means of sunshine duration (SD), wind speed (WS), relative humidity (RH) and maximum temperature (TMX) as predictors.

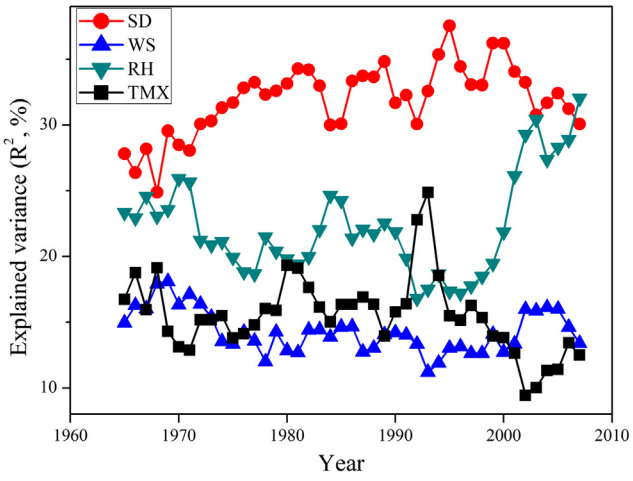

Fig. 5. Time series of explained variance EV (R^2,%) derived by stepwise multiple regression with annual reference crop evapotranspiration (ET_0) as dependent variable and annual means of sunshine duration (SD), wind speed (WS), relative humidity (RH) and maximum temperature (TMX) as predictors averaged for whole China with moving windows of ten years.

reaching EV similar to SD. Seasonal rankings however were more varied. Fig. 6 shows a pronounced seasonal distinction between spring and summer and autumn and winter, respectively. Spring and summer were dominated by SD explaining on average about 45 and 55% EV, respectively, with no distinct changes over time. In autumn and winter the situation was reversed with RH explaining on average about 35 and 45% EV, respectively. RH EV increased continuously during the last two decades reaching the level of summer SD.

4.2. Temporal and spatial variation of attribution

To illustrate spatial EV variability over time EV averaged over 4 time slices each covering 21 years are shown in Fig. 7. With the exception of TMX (EV range for a given area never exceeding 20%), all climatic variables showed pronounced variability, in some cases with an EV range of more than 50% for a given area. Superimposed at large scales, however, SD and WS EV showed a stable bisection along a meridional line running appr. at 105° E with high/low EV for SD in the east/west and vice versa for WS. Over the last 50 years the region of highest SD EV has moved northwards from the South China coast by more than 30° of latitude to extreme Northeast China. In a similar fashion the center of maximum WS EV moved to the south in Western China, but WS EV also decreased rapidly during the last two decades.

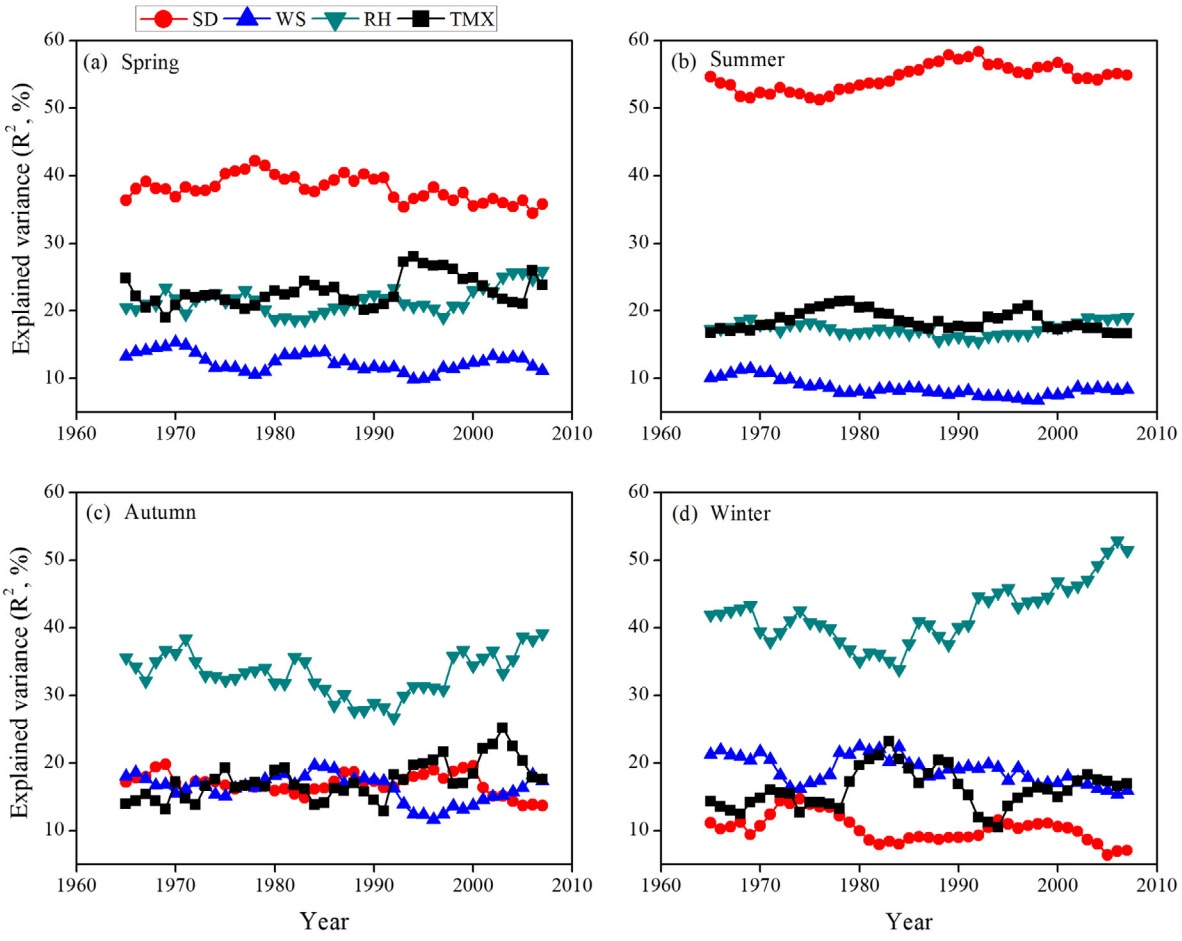

Fig. 6. Time series of explained variance EV (R^2,%) derived by stepwise multiple regression with seasonal reference crop evapotranspiration (ET_0) as dependent variable and seasonal means of sunshine duration (SD), wind speed (WS), relative humidity (RH) and maximum temperature (TMX) as predictors averaged for whole China with moving windows of ten years.

MFA analysis yielded 6 factors explaining a total variance of 46%. Out of these the first three each explained about 10% (Fig. 8). In contrast to the spatial arrangement of the EV of the input data (Fig. 7), most of the factors showed more zonal patterns. Particularly noteworthy are two linear structures in REOF #2 and #6 at appr. 27° N stretching through most of Southeast China. In contrast REOF #4 showed a patchy appearance with no obvious zonal patterns.

5. Discussion

Since the first publication on ET_0 trends over China (Thomas, 2000), numerous studies have confirmed that ET_0 trends are generally decreasing over China (for a review of AED trends both in China and abroad see McVicar et al. (2012)). China therefor fits in a global pattern of generally decreasing terrestrial ET_0 trends. Since China is a vast area with different climatic regions it is not surprising that spatial patterns of AED trends can be observed, namely with regard to the temporal regimes of different monsoonal circulation branches.

AED trends, however, did not change monotonically during the observation period. While trends mostly declined during the period 1960–1990, increasing trends were visible since the late 1990 s as reported by Gao et al. (2006) and Zhang et al. (2011a) for the whole of China as well as by Chen et al. (2006) and Zhang et al. (2009) for the Qinghai-Tibet Plateau. Chen et al. (2006) and Xing et al. (2016) suggest AED rates display decadal variations rather than monotonic changes. This is already an indication that the climatic variables influencing ET_0 rates also have to vary both in temporal and spatial terms. Our attribution study of ET_0 rates in Yunnan Province in Southwest China (Fan and Thomas, 2013) designed to analyze temporal variations of attribution has shown that attribution is highly variable over time both on an intra-annual and inter-annual variations level and between climatic variables. Seasonal variations appear to be linked to the change of properties and extent of monsoonal air masses in Southwest China.

5.1. Relationships between driving climatic factors and ET0 variability

Even though the decrease of SD, WS and RH in general has to lead to declining ET_0 rates both trend magnitude and the sensitivity of ET_0 to meteorological variables have to be taken into account together to arrive at an understanding of the driving mechanism of ET_0 rates. It is known that the sensitivity of ET_0 to meteorological variables also varies spatially (Fig. 4, Gong et al., 2006; Yin et al., 2010b; Zhang et al., 2011b). The decline of sunshine duration ('global dimming') is the main driving force for ET_0 decrease in tropical and subtropical China, which is consistent with the finding from subtropical and tropical humid region of China (Yin et al., 2010b; Stanhill and Cohen, 2001). In Southeast China the increase of aerosol concentrations accompanied with urbanization resulted in a decrease of net radiation that led to decreases in ET_0 rates (Liu et al., 2004; Zhang et al., 2011a).

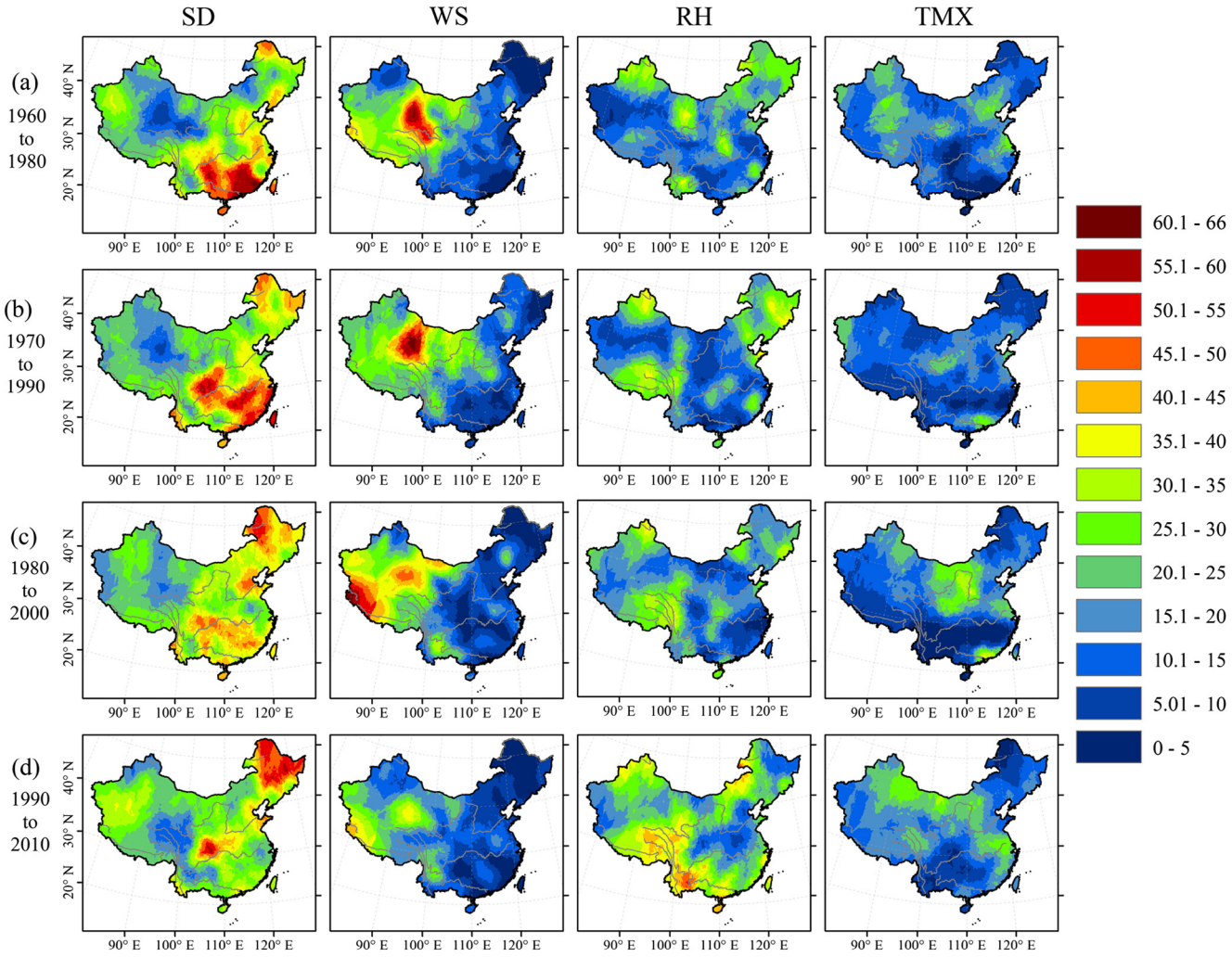

Fig. 7. Spatial patterns of explained variance EV (R^2,%) derived by stepwise multiple regression with annual reference crop evapotranspiration (ET_0) as dependent variable and annual means of sunshine duration (SD), wind speed (WS), relative humidity (RH) and maximum temperature (TMX) as predictors for four separated periods (1960–1980; 1970–1990; 1980–2000, 1990–2010) with a 21-year window.

Lower WS ('stilling') is the main cause of declining ET_0 rates in Northwest China (Fig. 4) which may be attributed to declining WS trends being higher in North China then in South China, and being higher in winter than in summer (Xu et al., 2006b; Wang et al., 2007; Guo et al., 2011; Zheng and Wang, 2014). The marked decrease of WS EV during the last five decades may be linked to a diminished monsoon circulation (Wang et al., 2004). RH was found to be most sensitive variable explaining ET_0 rates in the Yangtze River Basin (Gong et al., 2006). Our data however show no remarkable connection between RH and ET_0 rates in this region as – with the exception of the immediate coastal region - moderate negative RH trends combine with low EV. TMX always explained less than 25% of ET_0 rates. In the agricultural important Yangtze River basin, TMX EV even reached the lowest values in all of China indicating almost no influence on ET_0 rates. Although warm temperatures induce ET_0 to increase, mostly by lowering RH and providing energy input to the evaporating surface, temperature effects on ET_0 rates were negligible compared to other factors (Yin et al., 2010b).

5.2. Temporal and spatial variation of attribution

The above cited studies were all based on average values over their respective study periods and have not considered temporal changes of the relative importance of climatic variables for ET_0. In a pilot study in Yunnan Province in Southwest China we found that the attribution of climatic variables to ET_0 rates was not stable (Fan and Thomas, 2013). All-China EV time series (Figs. 5 and 6) show both long-term trends (such as a gradual rise and fall in SD EV), but also decadal scale changes such as the rapid rise of RH EV since the late 1990s may in winter. Both SD and RH are directly influenced by changes in precipitation and cloudiness, so varying EV values point to altered circulation patterns. Sea surface temperature and ENSO regimes are drivers of precipitation in East China (Ren et al., 2016; Zhang et al., 2016) with increased winter precipitation in South China since 1993 as reported by Ren et al. (2016). Both may have contributed to observed SD and RH EV changes.

Spatial SD, WS and to lesser extent RH EV patterns show a meridional division between East and West China at appr. 100°–105° E (Fig. 7). This is a well-known climatic division in South China between 'Indian' and 'Chinese' monsoon areas (Zhang, 1988) that further north defines the extent of the influence of maritime monsoonal air masses in China (Domrös and Peng, 1988). This bisection is again an indication that the large scale circulation is mirrored in spatial EV patterns: cloudiness and atmospheric water vapour content in Eastern China control SD while predominantly dry and cloudless conditions in Western China favor WS as dominant driver. Our finding is in line with Taban and Talaee

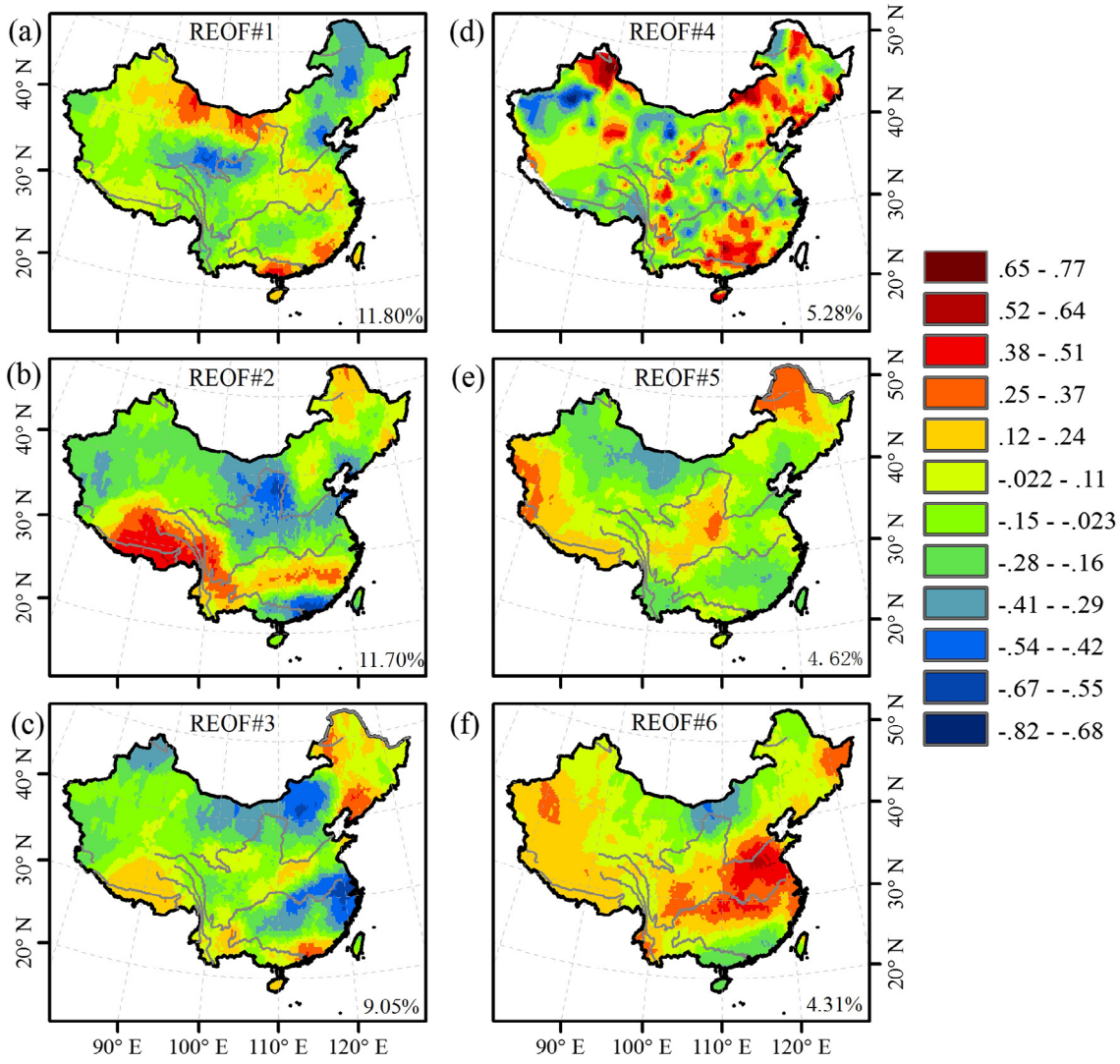

Fig. 8. Spatial distribution of factors 1 to 6 (REOF#1 to REOF#6) derived from multiple factor analysis (MFA) of time series of explained variance EV (R^2,%). Time series were derived by stepwise multiple regression with annual reference crop evapotranspiration (ET_0) as dependent variable and annual means of sunshine duration (SD), wind speed (WS), relative humidity (RH) and maximum temperature (TMX) as predictors for 644 stations. Percentage of explained variance for each factor is given in the lower right of each map.

(2014) who found that SD and WS dominate as drivers of ET in humid and arid climates, respectively.

We applied MFA to evaluate if an underlying spatial organization of EV can be found (Fig. 8). MFA reveals three major spatial patterns (REOF#1–REOF#3) that each explains about 10% of the total variance. Perhaps the most striking feature is the almost complete absence of the meridional division between East and West China visible in SD and WS EV in Fig. 7. Instead a zonal arrangement is apparent, REOF#2 shows this zonal pattern more clearly with a distinct band of high values along appr. 27° N in Southeast China. Both REOF#3 and REOF#6 show a sharp transition in the same region. This coincides with the region where most of the 'MeiYu' rainbands are initiated (Xu et al., 2009), a seasonal precipitation belt that forms in early summer in Southeast China. Precipitation and cloudiness as drivers of SD again point to the summer monsoon circulation as a possible decisive factor.

Compared to REOF#1–REOF#3 the patchy pattern of REOF#4 is an indicator of the influence of local factors which often are related to orography. This might indicate regions where orographic obstacles lead to cloud formation and dissipation on windward and leeward slopes, resp. Even though REOF#4 bears only a superficial resemblance to an orographic map of China low values in particular follow large scale depression such as the Tarim and Tengger desert basins in Northwest China and the Yangtze River valley in Southeast China.

For the allocation of water resources in the dominant rice growing areas of South China, but also for the irrigation planning in the wheat growing areas in North China, understanding and modelling the future amount and spatial distribution of ET rates is of crucial importance. ET_0 rates estimated from GCM results (e.g. Mo et al., 2013; Prudhomme and Williamson, 2013; Xing et al., 2014) are a key component for crop water balance calculations. Given our results GCM ET_0 rates based on formulations that do not include the effects of wind on ET have to be regarded with caution. Particularly in arid climates where wind speeds dominate attribution (Taban and Talaee, 2014) ET_0 rates in temperature-based models will depend mainly on the increasing temperature signal and consequently display rising instead of decreasing ET_0 rates such as in Terink et al. (2013).

Attribution of climatic variables can be considered a useful tool to verify if the underlying physics of a GCM model are able to reproduce the dependencies between ET_0 rates and forcing

climatic variables. Validation of GCM based ET_0 rates should therefore not only be able to reproduce the spatial organization of ET_0 rates, but also the spatio-temporal patterns of attribution. For century scale studies an adaption of the stomatal conductance value in the FAO-PM method to rising atmospheric CO_2 concentrations would have to be considered (Milly and Dunne, 2016). Besides finding that large uncertainties exist in future ET_0 projections using different GCMs, Xu et al. (2014) also note that 'the sensitivity of ET_0 based on GCM data in the baseline period is very different from that based on observations, indicating that the regional climate model did fail to preserve the sensitivity of ET_0 in the baseline period'. Even though the sensitivity of their simulated data in the future period was similar to that in the baseline period it is obvious that in such a case the resulting projections should be seen with caution.

6. Conclusion

Even though temperatures have increased, ET_0 and observed E_{pan} rates have in general been declining during the last decades, both in China and on a global scale. This contradicts the notion that ET_0 rates should increase in a warming climate. Decline of solar radiation rates ('global dimming') and wind speeds ('stilling') have been shown to be the main cause for decreased ET_0 rates.

The attribution of the four climatic variables SD, WS, RH and TMX to ET_0 rates in China varies geographically and on a seasonal basis. Maximum annual SD and WS EV are restricted to East and West China, respectively, while RH shows an irregular pattern of moderate EV. With the exception of Northwest China TMX EV are low throughout the study area. We inferred that the east–west division of SD and WS EV are the result of the monsoonal circulation with cloudiness governing SD variability in humid East China and WS dominating under mostly cloudless skies in arid West China.

The temporal evolution of annual EVs shows that with the exception of the last years SD EV always ranked highest and decreased only slightly during the last decade. In contrast RH EV experienced a rapid increase during the last two decades and reached SD levels in the last years due to an increase in winter. WS and TMX EVs remained on a low level and decreased slowly over the study period. An analysis of the temporal patterns of circulation parameters over East Asia *vs.* EV values should allow distinguishing the underlying causes of the observed changes.

Our results confirm that estimating ET_0 rates with simple temperature based estimation methods and without taking into account WS will likely give unreliable results, particularly in arid climates. For ET_0 estimates derived from GCM data, attribution analysis may be a helpful tool to assess the skill of GCM models.

Acknowledgments

We would like to thank Dr. Tim Hess, Cranfield University, who kindly provided us with Wasim-ET software. We thank three anonymous reviewers and the JoH editorial team for their constructive criticisms and valuable comments. Climate data were provided by the National Meteorological Information Centre of China (NMIC). This work was funded by the National Nature Science Foundation of China (No. 31770533, 31370496), National Key Research Development Program of China (2016YFC0502105) and Outstanding Young Research Fund of the Chinese Academy of Sciences.

Appendix A. Supplementary data

Supplementary data associated with this article can be found, in the online version, at https://doi.org/10.1016/j.jhydrol.2018.02.080.

References

Allen, R.G, Pereira, L.S, Raes, D., Smith, M. 1998. Crop evapotranspiration – Guidelines for Computing Crop Water Requirements. FAO Irrigation and Drainage Paper 56. Food and Agriculture Organization, Rome, Italy.

Ångström, A., 1924. Solar and terrestrial radiation. Quart. J. R. Meteorol. Soc. 50, 121–125.

Azorin-Molina, C., Vicente-Serrano, S.M., Sanchez-Lorenzo, A., McVicar, T.R., Morán-Tejeda, E., Revuelto, J., El Kenawy, A., Martín-Hernández, N., Tomas-Burguera, M., 2015. Atmospheric evaporative demand observations, estimates and driving factors in Spain (1961–2011). J. Hydrol. 523, 526–1277.

Brutsaert, W., Parlange, M.B., 1998. Hydrologic cycle explains the evaporation paradox. Nature 396, 30. https://doi.org/10.1038/23845.

Chen, D.L., Gao, G., Xu, C.Y., Guo, J., Ren, G.Y., 2005. Comparison of the Thornthwaite method and pan data with the standard Penman-Monteith estimates of reference evapotranspiration in China. Clim. Res. 28, 123–132.

Chen, S., Liu, Y., Thomas, A., 2006. Climatic change on the Tibetan Plateau: potential evapotranspiration trends from 1961–2000. Clim. Change 76, 291–319. https://doi.org/10.1007/s10584-006-9080-z.

Chen, R., Ersi, K., Yang, J., Lu, S., Zhao, W., 2004. Validation of five global radiation models with measured daily data in China. Energy Convers. Manage. 45, 1759–1769. https://doi.org/10.1016/j.enconman.2003.09.019.

Domrös, M., Peng, G.B., 1988. The Climate of China. Spinger-Verlag, Berlin, Germany.

Doorenbos, J., Pruitt, W.O. 1977. Guidelines for predicting crop water requirements. FAO Irrigation and Drainage Paper 24. Food and Agriculture Organization of the United Nations, Rome, Italy.

Escofier, B., Pages, J., 1994. Multiple factor analysis (AFMULT package). Computat. Statist. Data Anal. 18, 121–140.

ESRI, 2011. ArcGIS Desktop: Release 10. Environmental Systems Research Institute, Redlands, CA.

Fan, Z.X., Thomas, A., 2013. Spatiotemporal variability of reference evapotranspiration and its contributing climatic factors in Yunnan Province, SW China, 1961–2004. Clim. Change 116, 309–325. https://doi.org/10.1007/s10584-012-0479-4.

Fisher, J.B., Whittaker, R.J., Malhi, Y., 2011. ET come home: potential evapotranspiration in geographical ecology. Global Ecol. Biogeogr. 20, 1–18. https://doi.org/10.1111/j.1466-8238.2010.00578.x.

Gao, G., Chen, D., Ren, G., Chen, Y., Liao, Y., 2006. Spatial and temporal variations and controlling factors of potential evapotranspiration in China: 1956–2000. J. Geogr. Sci. 16, 3–12.

Gao, X., Peng, S., Wang, W., Xu, J., Yang, S., 2016. Spatial and temporal distribution characteristics of reference evapotranspiration trends in Karst area: a case study in Guizhou Province. China. Meteorol. Atmos. Phys. 128 (5), 677–688.

Gong, L., Xu, C.Y., Chen, D., Halldin, S., Chen, Y.D., 2006. Sensitivity of the Penman-Monteith reference evapotranspiration to key climatic variables in the Changjiang (Yangtze River) basin. J. Hydrol. 329, 620–629. https://doi.org/10.1016/j.jhydrol.2006.03.027.

Guijarro, J. 2014. User's Guide to Climatol V2.2. An R Contributed Package for Homogenization of Climatological Series. http://www.climatol.eu/index.html.

Guo, H., Xu, M., Hu, Q., 2011. Changes in near-surface wind speed in China: 1969–2005. Int. J. Climatol. 31, 349–358. https://doi.org/10.1002/joc.2091.

Hartmann, H., King, L., Jiang, T., Becker, S., 2009. Quasi-cycles in Chinese precipitation time series and in their potential influencing factors. Quat. Int. 208, 28–37. https://doi.org/10.1016/j.quaint.2008.10.011.

Huang, H., Han, Y., Cao, M., Song, J., Xiao, H., Cheng, W., 2015. Spatiotemporal characteristics of evapotranspiration paradox and impact factors in china in the period of 1960–2013. Adv. Meteorol. 4, 1–10. https://doi.org/10.1155/2015/519207.

Huntington, T.G., 2006. Evidence for intensification of the global water cycle: review and synthesis. J. Hydrol. 319, 83–95. https://doi.org/10.1016/j.jhydrol.2005.07.003.

IPCC. 2013. Summary for policymakers. In: Stocker, T.D., Qin, D., Plattner, G.K., Tignor, M., Allen, S.K., Boschung, J., Nauels, A., Xia, Y., Bex, V., Midgley, P.M. (eds.) Climate Change 2013: The Physical Science Basis. Contribution of Working Group I to the Fifth Assessment Report of the Intergovernmental Panel on Climate Change. Cambridge University Press, Cambridge, United Kingdom and New York, NY, USA. pp 1-29.

Lê, S., Josse, J., Husson, F., 2008. FactoMineR: An R package for multivariate analysis. J. Stat. Software 25, 1–18.

Li, X., Li, W., Zhou, X., 1998. Analysis of the solar radiation variation of China in recent 30 years. Quart. J. Appl. Meteorol. 9, 24–31.

Li, Z., Feng, Q., Liu, W., Wang, T., Gao, Y., Wang, Y., Cheng, A., Li, J., Liu, L., 2014. Spatial and temporal trend of potential evapotranspiration and related driving factors in southwest China, during 1961–2009. Quat. Int. 336, 127–144. https://doi.org/10.1016/j.quaint.2013.12.045.

Liu, B., Xu, M., Henderson, M., Gong, W., 2004. A spatial analysis of pan evaporation trend in China, 1955–2000. J. Geophy. Res. 109, D15102. https://doi.org/10.1029/2004JD004511.

Liu, B., Chen, X., Li, Y., Chen, X., 2017. Long-term change of potential evapotranspiration over southwest China and teleconnections with large-scale climate anomalies. J. Climatol. Int. https://doi.org/10.1002/joc.5309.

Liu, C., Zhang, D., Liu, X., Zhao, C., 2012. Spatial and temporal change in the potential evapotranspiration sensitivity to meteorological factors in China (1960–2007). J. Geogr. Sci. 22, 3–14. https://doi.org/10.1007/s11442-012-0907-4.

Liu, Q., Yang, Z.F., Cui, B.S., Sun, T., 2010. The temporal trends of reference evapotranspiration and its sensitivity to key meteorological variables in the Yellow River Basin China. Hydrol. Proc. 24, 2171–2181. https://doi.org/10.1002/hyp.7649.

Milly, P.C.D., Dunne, K.A., 2016. Potential evapotranspiration and continental drying. Nat. Clim. Change 6, 946–949. https://doi.org/10.1038/nclimate3046.

McVicar, T.R., Roderick, M.L., Donohue, R.J., Li, L.T., Van Niel, T.G., Thomas, A., Grieser, J., Jhajharia, D., Himri, Y., Mahowald, N.M., Mescherskaya, A.V., Kruger, A.C., Rehman, S., Dinpashoh, Y., 2012. Global review and synthesis of trends in observed terrestrial near-surface wind speeds: Implications for evaporation. J. Hydrol. 416–417, 182–205. https://doi.org/10.1016/j.jhydrol.2011.10.024.

Mo, X., Guo, R., Liu, S., Lin, Z., Hu, S., 2013. Impacts of climate change on crop evapotranspiration with ensemble GCM projections in the North China Plain. Clim. Change 120, 299–312. https://doi.org/10.1007/s10584-013-0823-3.

Monteith, J.L., 1965. Evaporation and Environment. Symp. Soc. Exp. Biol. 19, 205–234.

Penman, H.L., 1948. Natural evaporation from open water, bare soil and grass. Proc. R. Soc. Lon. A 193, 120–145.

Peterson, T.C., Easterling, D.R., Karl, T.R., Groisman, P., Nicholls, N., Plummer, N., Torok, S., Auer, I., Böhm, R., Gullett, D., Vincent, L., Heino, R., Tuomenvirta, H., Mestre, O., Szentimrey, T., Salinger, J., Førland, E.J., Hanssen-Bauer, I., Alexandersson, H., Jones, P., Parker, D., 1998. Homogeneity adjustments of situ atmospheric climate data: a review. Int. J. Climatol. 18, 1493–1517.

Peterson, T.C., Golubev, V.S., Groisman, P.Y., 1995. Evaporation losing its strength. Nature 377, 687–688. https://doi.org/10.1038/377687b0.

Piao, S.L., Ciais, P., Huang, Y., Shen, Z.H., Peng, S.S., Li, J.S., Zhou, L.P., Liu, H.Y., Ma, Y. C., Ding, Y.H., Friedlingstein, P., Liu, C.Z., Tan, K., Yu, Y.Q., Zhang, T.Y., Fang, J.Y., 2010. The impacts of climate change on water resources and agriculture in China. Nature 467, 43–51. https://doi.org/10.1038/nature09364.

Prudhomme, C., Williamson, J., 2013. Derivation of RCM-driven potential evapotranspiration for hydrological climate change impact analysis in Great Britain: a comparison of methods and associated uncertainty in future projections. Hydrol. Earth Syst. Sci. 17, 1365–1377.

R Development Core Team. 2004. R: A Language and Environment for Statistical Computing. R Foundation for Statistical Computing, Vienna

Ren, Q., Zhu, Z., Hao, L., He, J., 2016. The enhanced relationship between Southern China winter rainfall and warm pool ocean heat content. Int. J. Climatol. 37 (1), 409–419. https://doi.org/10.1002/joc.4714.

Roderick, M.L., Farquhar, G.D., 2002. The cause of decreased pan evaporation over the past 50 years. Science 298 (5597), 1410–1411.

Roderick, M.L., Hobbins, M.T., Farquahar, G.D., 2009. Pan evaporation trends and the terrestrial water balance I. Principles and observations. Geograp. Comp. 3, 746–760. https://doi.org/10.1111/j.1749-8198.2008.00213.x.

Scheff, J., Frierson, D.M.W., 2014. Scaling potential evapotranspiration with greenhouse warming. J. Clim. 27, 1539–1558. https://doi.org/10.1175/JCLI-D-13-00233.1.

Shuttleworth, W.J., 1993. Evaporation. In: Maidment, D.R. (Ed.), Handbook of Hydrology. McGraw-Hill, Sydney.

Smith, L.P., 1975. Methods in agricultural meteorology. Developments in Atmospheric Science. Elsevier, Oxford.

Song, Z.W., Zhang, H.L., Snyder, R.L., Anderson, F.E., Chen, F., 2010. Distribution and trends in reference evapotranspiration in the North China Plain. J. Irrig. Drain. Eng. 136, 240–247.

Stanhill, G., Cohen, S., 2001. Global dimming: A review of the evidence for a widespread and significant reduction in global radiation with discussion of its probable causes and possible agricultural consequences. Agr. Forest Meteorol. 107, 255–278. https://doi.org/10.1016/S0168-1923(00)00241-0.

Taban, H., Talaee, P.H., 2014. Sensitivity of evapotranspiration to climate change in different climates. Global Planet. Change 115, 16–23.

Tang, B., Tong, L., Kang, S., Zhang, L., 2011. Impacts of climate variability on reference evapotranspiration over 58 years in the Haihe river basin of north China. Agric. Water Manage. 98, 1660–1670. https://doi.org/10.1016/j.agwat.2011.06.006.

Terink, W., Immerzeel, W.W., Droogers, P., 2013. Climate change projections of precipitation and reference evapotranspiration for the Middle East and Northern Africa until 2050. Int. J. Climatol. 33, 3055–3072.

Thomas, A., 2000. Spatial and temporal characteristics of potential evapotranspiration trends over China. Int. J. Climatol. 20, 381–396.

Vautard, R., Cattiaux, J., Yiou, P., Thepaut, J.-N., Ciais, P., 2010. Northern Hemisphere atmospheric stilling partly attributed to an increase in surface roughness. Nat. Geosci. 3, 756–761. https://doi.org/10.1038/ngeo979.

Wang, Z., Ding, Y., He, J., Yu, J., 2004. An updating analysis of the climate change in China in recent 50 years. Acta Meteorol. Sin. 62, 228–236.

Wang, Z.Y., Jiang, T., Bothe, O., Fraedrich, K., 2007. Changes of pan evaporation and reference evapotranspiration in the Yangtze River basin. Theor. Appl. Climatol. 90, 13–23. https://doi.org/10.1007/s00704-006-0276-y.

Wang, W.G., Peng, S.Z., Yang, T., Shao, Q.X., Xu, J.Z., Xing, W.Q., 2011. Spatial and temporal characteristics of reference evapotranspiration trends in the Haihe River basin China. J. Hydrol. Eng. 16, 239–252.

Wang, Z., Xie, P., Lai, C., Chen, X., Wu, X., Zeng, Z., Li, J., 2017. Spatiotemporal variability of reference evapotranspiration and contributing climatic factors in China during 1961–2013. J. Hydrol. 544, 97–108.

Wild, M., Gilgen, H., Roesch, A., Ohmura, A., Long, C.N., Dutton, E.G., Forgan, B., Kallis, A., Russak, V., Tsvetkov, A., 2005. From dimming to brightening: decadal changes in solar radiation at earth's surface. Science 308, 847–850. https://doi.org/10.1126/science.1103215.

Xing, W., Wang, W., Shao, Q., Peng, S., Yu, Z., Yong, B., Taylor, J., 2014. Changes of reference evapotranspiration in the Haihe River Basin: Present observations and future projection from climatic variables through multi-model ensemble. Global Planet. Change 115, 1–15.

Xing, W., Wang, W., Shao, Q., Yu, Z., Yang, T., Fu, J., 2016. Periodic fluctuation of reference evapotranspiration during the past five decades: Does Evaporation Paradox really exist in China? Sci. Rep. 6, 39503. https://doi.org/10.1038/srep39503.

Xu, C.Y., Gong, L., Jiang, T., Chen, D., Singh, V.P., 2006a. Analysis of spatial distribution and temporal trend of reference evapotranspiration and pan evaporation in Changjiang (Yangtze River) catchment. J. Hydrol. 327, 81–93. https://doi.org/10.1016/j.jhydrol.2005.11.029.

Xu, M., Chang, C.P., Fu, C., Qi, Y., Robock, A., Robinson, D., Zhang, H.M., 2006b. Steady decline of east Asian monsoon winds, 1969–2000: Evidence from direct ground measurements of wind speed. J. Geophys. Res. 111, D24111. https://doi.org/10.1029/2006JD007337.

Xu, W., Zipser, E.J., Liu, C., 2009. Rainfall characteristics and convective properties of Mei-Yu precipitation systems over South China, Taiwan, and the South China sea. Part I: TRMM observation. Mon. Wea. Rev. 13, 4261–4275. https://doi.org/10.1175/2009MWR2982.1.

Xu, Y.P., Pan, S., Fu, G., Tian, Y., Zhang, X., 2014. Future potential evapotranspiration changes and contribution analysis in Zhejiang Province, East China. J. Geophys. Res. 118, 2174–2192. https://doi.org/10.1002/2013JD021245.

Ye, X., Li, X., Liu, J., Xu, C.-Y., Zhang, Q., 2014. Variation of reference evapotranspiration and its contributing climatic factors in the Poyang Lake catchment. China. Hydrol. Process. 28, 6151–6162.

Yin, Y., Wu, S., Chen, G., Dai, E., 2010a. Attribution analyses of potential evapotranspiration changes in China since the 1960s. Theor. Appl. Climatol. 101, 9–28. https://doi.org/10.1007/s00704-009-0197-7.

Yin, Y., Wu, S., Dai, E., 2010b. Determining factors in potential evapotranspiration changes over China in the period 1971–2008. Chin. Sci. Bull. 55, 3329–3337. https://doi.org/10.1007/s11434-010-3289-y.

Zhang, K., 1988. The climatic dividing line between SW and SE Monsoons and their differences in climatology and ecology in Yunnan Province of China. Climatol. Note. 38, 157–166.

Zhang, Q., Xu, C.Y., Chen, X., 2011a. Reference evapotranspiration changes in China: natural processes or human influences? Theor. Appl. Climatol. 103, 479–488. https://doi.org/10.1007/s00704-010-0315-6.

Zhang, Q., Wang, Y., Singh, V.P., Gu, X., Kong, D., Xiao, M., 2016. Impacts of ENSO and ENSO Modoki+A regimes on seasonal precipitation variations and possible underlying causes in the Huai River basin China. J. Hydrol. 533, 308–319. https://doi.org/10.1016/j.jhydrol.2015.12.003.

Zhang, S., Liu, S., Mo, X., Shu, C., Sun, Y., Zhang, C., 2011b. Assessing the impact of climate change on potential evapotranspiration in Aksu River Basin. J. Geogr. Sci. 21, 609–620. https://doi.org/10.1007/s11442-011-0867-0.

Zhang, X., Ren, Y., Yin, Z.Y., Lin, Z., Zheng, D., 2009. Spatial and temporal variation patterns of reference evapotranspiration across the Qinghai-Tibetan Plateau during 1971–2004. J. Geophys. Res. 114, D15105. https://doi.org/10.1029/2009JD011753.

Zhang, Y.Q., Liu, C.M., Tang, Y.H., Yang, Y.H., 2007. Trends in pan evaporation and reference and actual evapotranspiration across the Tibetan Plateau. J. Geophys. Res. 112, D12110. https://doi.org/10.1029/2006JD008161.

Zheng, H., Liu, X., Liu, C., Dai, X., Zhu, R., 2009. Assessing contributions to pan evaporation trends in Haihe River Basin China. J. Geophys. Res. 114, D24105. https://doi.org/10.1029/2009JD012203.

Zheng, C., Wang, Q., 2014. Spatiotemporal variations of reference evapotranspiration in recent five decades in the arid land of Northwestern China. Hydrol. Proc. 28, 6124–6134. https://doi.org/10.1002/hyp.10109.

Zheng, C., Wang, Q., 2015. Spatiotemporal pattern of the global sensitivity of the reference evapotranspiration to climatic variables in recent five decades over China. Stoch. Environ. Res. Risk Assess. 29, 1937. https://doi.org/10.1007/s00477-015-1120-7.